Electronic Supplementary Material (ESI) for ChemComm.
This journal is © The Royal Society of Chemistry 2018

Supplementary information

Alkali-Induced Crumpling of $Ti_3C_2T_x$ (MXene) to Form 3D Porous Networks for Sodium Ion Storage

Di Zhao,[a] Mallory Clites,[a] Guobing Ying,[a] Sankalp Kota,[a] Jie Wang,[b] Varun Natu,[a] Xin Wang,[b] Ekaterina Pomerantseva,[a] Minhua Cao,*[b] and Michel W. Barsoum*[a]

[a] Department of Materials Science and Engineering, Drexel University, Philadelphia, PA 19104

[b] Key Laboratory of Cluster Science, Ministry of Education of China, Beijing Key Laboratory of Photoelectronic/Electrophotonic Conversion Materials, School of Chemistry and Chemical Engineering, Beijing Institute of Technology, Beijing 100081, P. R. China.

Experimental Details

Preparation of Ti_3AlC_2.

Powders of Ti_3AlC_2 were was prepared by mixing commercial Ti_2AlC powders (Kanthal, Sweden) with TiC in a 1:1 molar ratio (after adjusting for the ≈ 10 wt% Ti_3AlC_2 already present in the commercial powder) followed by ball milling for 1 day. The mixture was placed in an alumina boat and heated at a rate of 5 °C/min under continuous Ar flow to 1350 °C and held at that temperature for 2 h. The resulting loosely sintered brick was ground with a TiN-coated milling bit and sieved through a 400 mesh sieve producing a powder with a particle size less < 38 µm.

Preparation of delaminated $Ti_3C_2T_x$ MXene suspension

Typically, 0.99 g of LiF (Alfa Aesar, 98.5%) was dissolved in 10 mL of 12 M HCl. Then 1 g of sieved Ti_3AlC_2 powders was added. The mixture was kept at 35 °C for 24 h while stirring with a magnetic stirrer. The resulting solid residue was washed several times with deionized water and centrifuged at a speed of 3500 rpm (3 min for each cycle) until the pH of the supernatant was about 6. The resulting powder was mixed with about 40 ml of distilled water and sonicated for 1 h under an ice-bath through which Ar gas was bubbled. The resulting solution was centrifuged for 40 min at a speed of 3500 rpm. Finally, the supernatant colloidal suspension, containing delaminated, mostly single, 2D $Ti_3C_2T_x$ flakes, was obtained.

To determine the volumetric density, a syringe was used to pull out 3 ml of the colloidal suspension to filter a film. The remaining suspension was stored in sealed bottles under Ar for further experiments. After drying in air, weighed it. For all the work carried out herein, the as-produced $Ti_3C_2T_x$ MXene solution concentration was about 15 mg ml^{-1}.

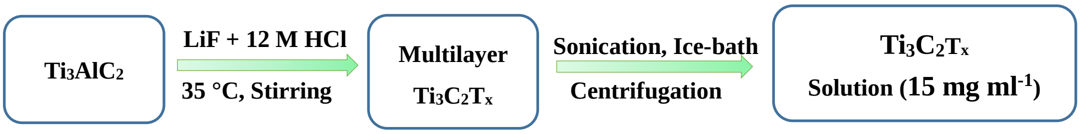

Scheme S1. Preparation steps for MXene nanosheets.

Electrostatic assembly of $Ti_3C_2T_x$ with cations.

The ≈ 15 mg ml^{-1} colloidal suspension was then mixed, at room temperature, with 1 M solutions of KOH, LiOH and NaOH. And also mixed with NH_4OH (25~28%) and TBAOH (1.5 M). For 2 ml MXene solution, adding about 2 ml alkaline solutions. This resulted in the immediate flocculation of the $Ti_3C_2T_x$ nanosheets. The flocculated deposit was separated from its solution by centrifugation. They were then washed with water one time and ethanol until neutral without shaking very strongly. The resulting materials were dried in a dryer.

Materials Characterization

Powder X-ray diffraction (XRD) was performed on a Rigaku Smart Lab (Tokyo, Japan) diffractometer using Cu Kα radiation (40 KV and 44 mA) and step scan 0.02°, 3°-65° 2 theta range and a step time of 0.5 s.

The zeta, ζ, potential measurements were conducted using a Zetasizer Nano ZS apparatus from Malvern Instruments. First, we ground the flocculation products in a mortar and pestle, and then dispersed a small amount in water solution using ultrasound. Finally, getting about 280 µl using microsyringe to test it.

The structure and morphology of the materials were examined with Scanning Electron

Microscopy (SEM), Energy-Dispersive Spectroscopy (EDS) and Transmission electron microscopy (TEM). SEM and EDS were performed on a Zeiss Supra 50VP (Carl Zeiss AG, Germany). The TEM was a JEOL JEM-2010.

Atomic force microscopy (AFM) images were obtained by Bruker DI MultiMode-8 system under tapping mode. First, we ground the flocculation products into a fine powder and then dispersed a little of it in water under ultrasound. Water was then added to about 2 ml of supernatant to create a very dilute suspension. A drop of that dilute suspension was dropped on a clean mica sheet, and its thickness was measured.

BrunauereEmmeteTeller (BET) isotherms and specific surface area (BET surface area) were performed on a Kubo X1000 instrument at 77 K. Pore size distribution and pore volume were derived using the analysis methods of BarretteJoynereHalenda (BJH).

Electrochemical Measurements of *c*-$Ti_3C_2T_x$ as a Na Ion Electrode: The electrochemical tests were performed at room temperature using coin cells (CR2025) on LAND CT2001A, with a cutoff voltage of 0.01-3.00 V *vs.* Na/Na^+.

The anodes were prepared by mixing, dried Na-*c*-$Ti_3C_2T_x$ powders, conductive carbon black, and sodium carboxymethyl cellulose (CMC) in a 80:10:10 weight ratio in a mortar and pestle. Deionized water was used as the solvent to make a homogeneous slurry. The resulting slurry was uniformly pasted on a Cu foil and dried at 60 °C for 12 h and then at 120 °C for another 12 h in a vacuum oven. Final cell assembly was carried out in an Ar-filled glovebox.

The loading of the active material was about 0.8 mg cm^{-2}. Here Na metal functioned as both counter and reference electrodes. A 1 M $NaClO_4$ in a mixture of EC/dimethyl carbonate (1:1 by volume) with 5 wt.% fluoroethylene carbonate (FEC) acted as the electrolyte. The galvanostatic charge/discharge performance was investigated with a voltage cut off of 0.01-3.00 V (*vs.* Na/Na^+). CV curves were measured by a CHI-760E electrochemical workstation with a scan rate of 0.2 mV s^{-1}.

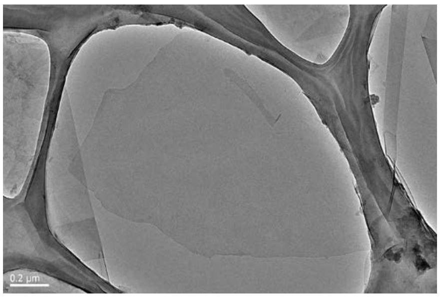

Fig. S1 Typical TEM image of exfoliated $Ti_3C_2T_x$ nanosheets produced by sonication.

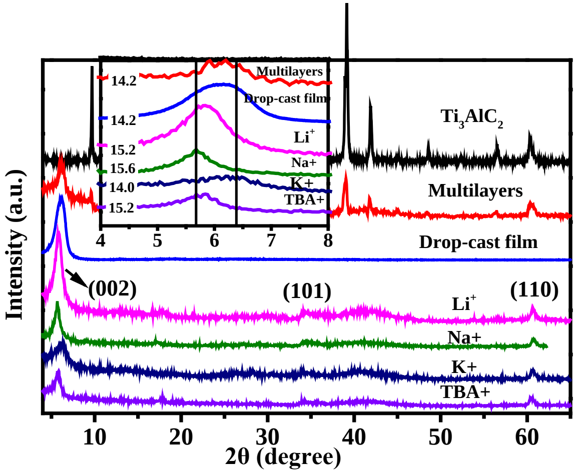

Fig. S2 XRD patterns of (from top to bottom) Ti_3AlC_2, $Ti_3C_2T_x$ multilayers, drop cast film, Li-*c*-$Ti_3C_2T_x$, Na-*c*-$Ti_3C_2T_x$, K-*c*-$Ti_3C_2T_x$ and, TBA-*c*-$Ti_3C_2T_x$. Note peak at 2θ ≈ 61° in all but c. Inset shows low angle results. The numbers in inset are the $d_{c/2}$ values calculated from the (002) peak positions. They fall in two groups, separated by ≈ 1 Å. Vertical lines in inset are guides to the eyes.

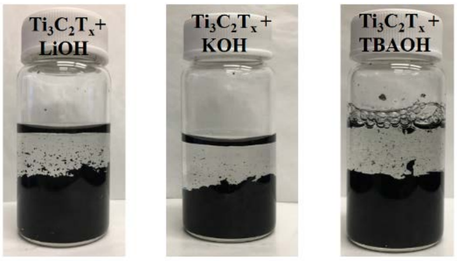

Fig. S3 Pictures of flocculation products obtained when $Ti_3C_2T_x$ colloidal solutions after the addition of LiOH, KOH and TBAOH.

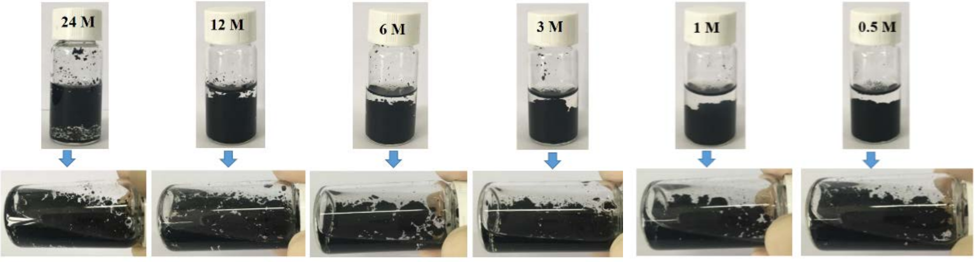

Fig. S4 Photograph of Na-$Ti_3C_2T_x$ 3D framework with different NaOH concentrations from 0.5 M to 24 M. In all cases, the $Ti_3C_2T_x$ flakes readily flocculated and crashed out of solution.

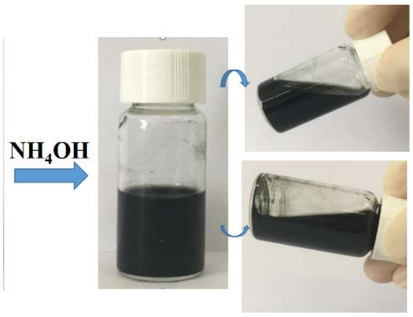

Fig. S5 Photographs showing absence of flocculation when NH_4OH is added to a $Ti_3C_2T_x$ colloidal solution.

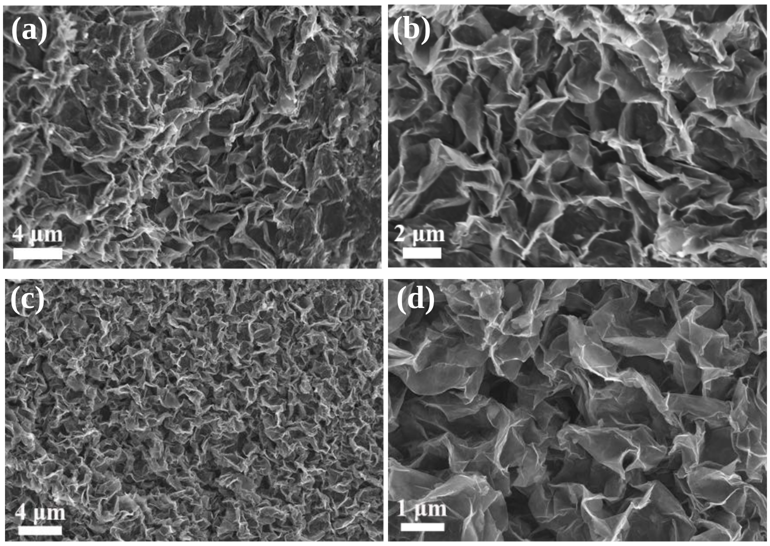

Fig. S6 Low and high magnification SEM micrographs of products obtained when (a,b) LiOH and (c,d) KOH solutions are added to a colloidal suspension of $Ti_3C_2T_x$.

(a)

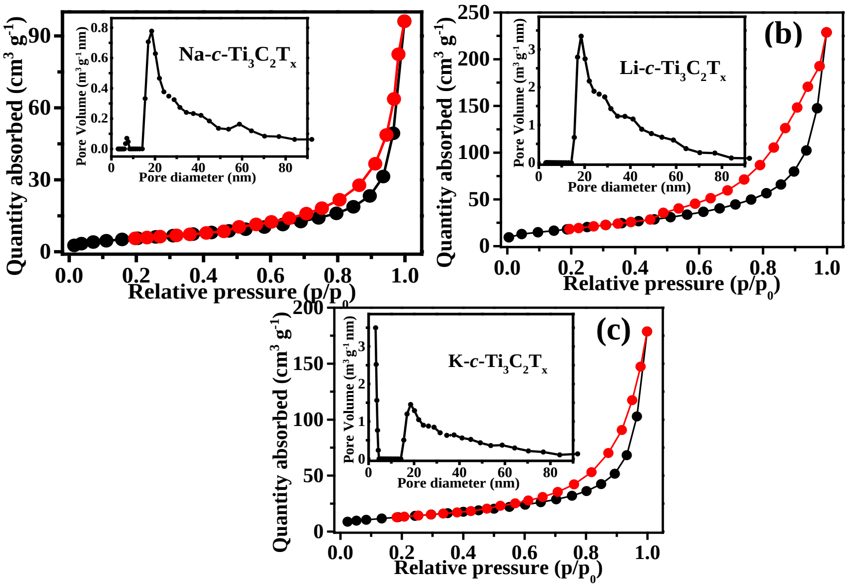

Fig. S7 (a,b,c) N_2 adsorption–desorption isotherms and pore distribution curves calculated by the NLDFT method for, a) Na-*c*-$Ti_3C_2T_x$, b) Li-*c*-$Ti_3C_2T_x$ and, c) K-*c*-$Ti_3C_2T_x$.

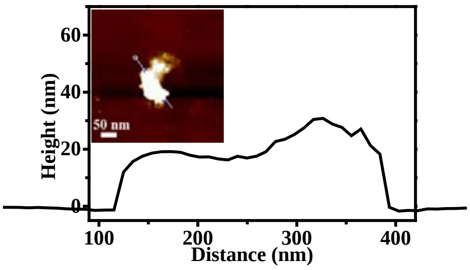

Fig. S8 Height profile measured along the white line shown in inset AFM image.

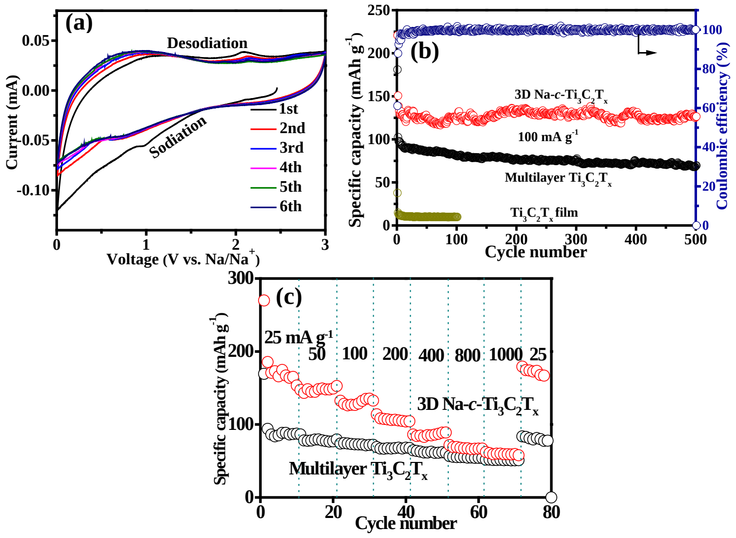

Fig. S9 (a) CV curves of Na-*c*-$Ti_3C_2T_x$ at a scan rate of 0.2 mV s^{-1}. (b) Cycling stability of Na-*c*-$Ti_3C_2T_x$, ML-$Ti_3C_2T_x$ and $Ti_3C_2T_x$ film electrodes at a current density of 100 mA g^{-1}. (c) Rate performance of Na-*c*-$Ti_3C_2T_x$ and ML-$Ti_3C_2T_x$ electrodes.

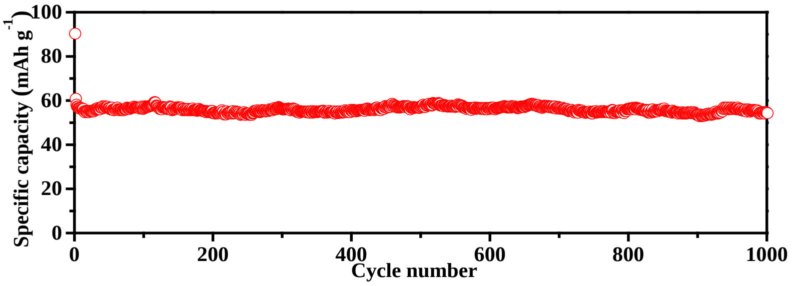

Fig. S10 Cycling performance at a current density of 1.5 A g^{-1} for Na-*c*-$Ti_3C_2T_x$.

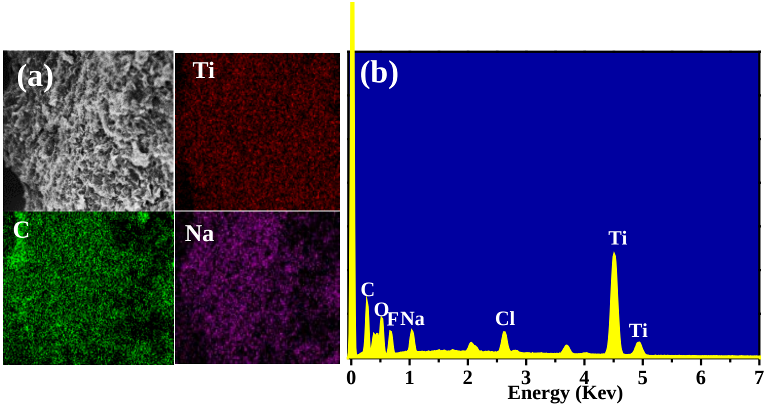

Fig. S11 (a) SEM image and elemental maps of Ti, C and Na in Na-*c*-$Ti_3C_2T_x$ flocculated network. (b) EDS spectrum of Na-$Ti_3C_2T_x$ flocculation with NaOH solution.

Table S1 Elements contents of Na-$Ti_3C_2T_x$ flocculation with NaOH solution getting from EDS spectrum.

Elements	C	O	F	Na	Cl	Ti	Total
wt%	9.18	11.92	6.43	2.34	3.56	66.58	100.00
Atomic ratio (%)	22.22	21.66	9.84	2.96	2.92	40.41	100.00

Table S2 Comparison of the capacity of 3D Na-*c*-$Ti_3C_2T_x$ in this work with those of other reported $Ti_3C_2T_x$ or other MXene materials as anodes for SIBs.

Materials	Capacity [mAh g^{-}]	Current density [mA g^{-1}]	Cycle number	Year	Ref.	
3D Na-*c*-$Ti_3C_2T_x$	151 130 54	25 100 1500	10 500 1000			
3D Li-*c*-$Ti_3C_2T_x$	200200 167167	100100 100100	**100**100 300 100300	ThisThis work work	100 300	This w
3D K-*c*-$Ti_3C_2T_x$	100100 105105	100 100100 100 100	100 100 300 300			
Multilayer $Ti_3C_2T_x$	79	100	120	2014	1	
Na^+ insertion multilayer $Ti_3C_2T_x$	100	20	100	2016	2	

Alkalized $Ti_3C_2T_x$ nanoribbons	113	50	200	2017	3
	53	200	500		
$Ti_3C_2T_x$ MXene	100	50	200	2015	4
	68.3	200	1000		
Hollow $Ti_3C_2T_x$ spheres	210	500	1000	2017	5
Hollow Mo_2CT_x spheres	210	500	1000		
Multilayer V_2CT_x	75	30	50	2015	6
	67	30	100		
Ti_2CT_x	143	20	100	2015	7

Table S3 Comparison of $d_{c/2}$ values in Å, for 3D Na-*c*-$Ti_3C_2T_x$ measured in this work and those reported cations intercalated $Ti_3C_2T_x$ MXene.

Materials	c-LP (Å)	Ref.
3D Na-c-$Ti_3C_2T_x$	15.6	This work
Ti_3C_2 MXene nanoribbons	12.5	3
Cations intercalated MXene with		
KOH	10.15	8
NH_4OH	12.7	8
Ti_2CT_x	10.1	7
$Ti_3C_2T_x$ treated with Hydrazine	12.74	9
$Ti_3C_2T_x$ treated in DMF	13.4	9
MXene $Ti_3C_2T_x$ in a nonaqueous Na^+ electrolyte	12.5	2

References

(1) Y. Xie, Y. Dall’Agnese, M Naguib,.,Y. Gogotsi, M. W. Barsoum, H. L. Zhuang, P. R. C. Kent, *ACS nano,* 2014, **8**, 9606–9615.

(2) S. Kajiyama, L. Szabova, K. Sodeyama, H. Iinuma, R. Morita, K. Gotoh, Y. Tateyama, M. Okubo, A. Yamada, *ACS Nano,* 2016, **10**, 3334-3341.

(3) P. Lian, Y. Dong, Z. S. Wu, S. Zheng, X. Wang, W. Sen, C. Sun, J. Qin, X. Shi, X. Bao, *Nano Energy,* 2017, **40**, 1-8.

(4) X. Wang, X. Shen, Y. Gao, Z. Wang, R. Yu, L. Chen, *J. Am. Chem. Soc.*, 2015, **137**, 2715-2721.

(5) M. Q. Zhao, X. Xie, C. E. Ren, T. Makaryan, B. Anasori, G. Wang, Y. Gogotsi, *Adv. Mater.*, 2017, **29**,1702410.

(6) Y. Dall'Agnese, P. L. Taberna, Y. Gogotsi, P. Simon, *J. Phys. Chem. Lett.*, 2015, **6**, 2305-2309.

(7) X. Wang, S. Kajiyama, H. Iinuma, E. Hosono, S. Oro, I. Moriguchi, M. Okubo, A. Yamada, *Nat. Commun.*, 2015, **6**, 6544.

(8) M. R. Lukatskaya, O. Mashtalir, C. E. Ren, Y. Dall’Agnese, P. Rozier, P. L. Taberna, M. Naguib, P. Simon, M. W. Barsoum, Y. Gogotsi. *Science,* 2013, **341**, 1502-1505.

(9) O. Mashtalir, M. Naguib, V. N. Mochalin, Y. Dall'Agnese, M. Heon, M. W. Barsoum, Y. Gogotsi, *Nat. Commun.*, 2013, **4**, 1716.